JOURNAL OF MATERIALS SCIENCE 33 (1998) 1431–1440

Deformation characteristics of metal foams

J. BANHART, J. BAUMEISTER
Fraunhofer Institute for Applied Materials Research, Lesumer Heerstraße 36, 28717 Bremen, Germany
E-mail: ban@ifam.fhg.de

The deformation behaviour of a series of aluminium and zinc foams was investigated by uniaxial testing. Because the deformation behaviour of metal foams is expected to be anisotropic owing to the existence of a closed outer skin and with respect to the foaming direction, a series of measurements was carried out where the orientation of the outer skin and the foaming direction were varied. Stress–strain diagrams and corresponding compression strengths were determined for aluminium- and zinc-based foams. The influence of an age-hardening heat treatment was investigated. Finally, the axial deformation behaviour of aluminium tubes filled with aluminium foam was tested under uniaxial loading conditions. The results of the measurements are discussed in the context of possible applications of metal foams as energy absorbers. © *1998 Chapman & Hall*

1. Introduction

In the past few years there has been a considerable increase in interest for metal foams, especially made of aluminium or aluminium alloys. The reasons for this are recent process developments which promise a better quality of the foamed material. Moreover, the conditions for the application of new materials have changed very much. Increased demands concerning passenger safety in automobiles or materials recycling make constructors now think of using metal foams where a few years ago the same material would have been ruled out for technical or economic reasons.

One reason for the fact that metal foams have not become very popular yet are the manufacturing processes which were available in the past. They were characterized by relatively high costs and a poor quality of the foamed material. In the last 10 years there has been quite some improvement in this respect, so that nowadays various methods for making metal foams are available, some starting from the molten metal [1–3], and others from metal powders [1, 4–8]. In particular, a powder method for foaming metals was invented a few years ago at the Fraunhofer Institute. It allows for the production of foamed metals based on aluminium, zinc, tin, lead and alloys thereof [1, 4–8].

There are many possible applications for metal foams ranging from light-weight construction, sound and heat insulation to energy absorption applications. The latter makes use of the combination of high strength and the characteristic non-linear deformation behaviour, which originates from the cellular nature of metal foams. It is therefore an important task to characterize the deformation behaviour of metal foams to be able to assess the application opportunities. A general overview over the mechanical properties of foamed structures can be found in [9]. The compression of aluminium foams has been investigated by Thornton and Magee [10, 11] about 20 years ago and recently by the present authors [12–14]. In this paper we carry on the existing characterization of metal foam systems. Because in most real applications the bare metal foam will not be used but some kind of composite structure is desired, we extend the work to very simple composites consisting of the foam and a closed outer hull. The hull may be the densified skin, which is created during foaming or a massive aluminium tube which is filled with aluminium foam in a special modification of the foaming process.

2. Sample preparation

Metal foam was produced by the powder-metallurgical Fraunhofer process. The process is described schematically in Fig. 1; aluminium and zinc alloys were prepared by mixing metal powders in the appropriate relations. The foaming agent titanium hydride or zirconium hydride was then added to this mixture. The foaming agent content depends on the metal to be foamed and the desired density and range from 0.4 to 0.8 wt % in the present case. The mixture containing the agent was then compacted by extrusion (Al) or axial compaction (Zn). As a result a semifinished product is obtained in which the foaming agent is homogeneously distributed within a dense, virtually non-porous metallic matrix. This foamable material was processed into pieces of the desired size and shape by rolling and cutting. Finally, foamed metal parts were obtained by heating the material to temperatures above the melting point of the matrix metal. The metal melts and the foaming agent releases gas in a controlled way, so that the metal transforms into semisolid foamy mass which expands slowly. The foaming took place inside simple closed moulds which were then completely filled by the foam. After the mould had been filled, the process was stopped by simply

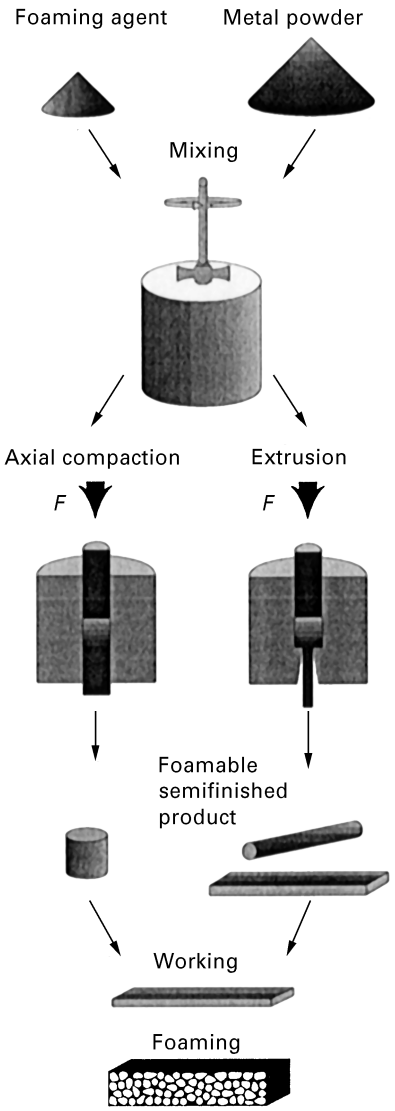

Figure 1 Powder process for making metal foams [4–8].

allowing the mould to cool to a temperature below the melting point of the metal. The density of the metal foams was controlled by adjusting the content of foaming agent and varying the heating conditions. The resulting foamed body has a closed outer skin. If the body is cut apart, the highly porous structure becomes evident (Fig. 2). The aluminium foams were made from a powder mixture of the nominal composition Al–6 wt % Si–4 wt % Cu, the zinc foams from Zn–4 wt % Cu mixtures.

For the compression testing of aluminium foams, rectangular foamed blocks having the dimensions 130 mm × 100 mm × 40 mm were manufactured by filling an appropriate rectangular mould. The blocks were cut into six pieces, each of which had the dimensions 40 mm × 40 mm × 40 mm and densities ranging from 0.2 to 0.8 g cm^{-3} (Fig. 3). Each sample then showed two faces with a closed outer skin and four faces which were open. The samples for the characterization of zinc foams were foamed inside a cylindrical mould with a diameter of 30 mm and 40 mm length. The resulting samples were also cylindrical, and all faces and sides remained closed.

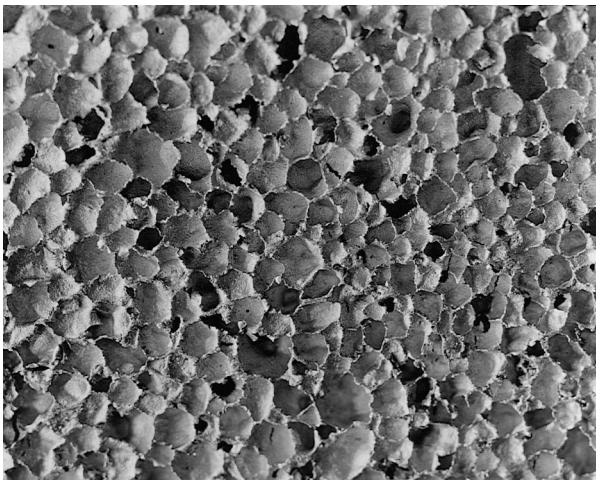

Figure 2 Pore structure of an aluminium foam (area of photograph, 60 mm × 50 mm).

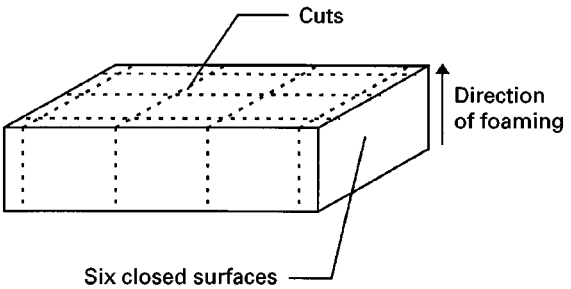

Figure 3 Preparation of aluminium foam test samples from a foam block.

The aluminium foams were all heat treated after foaming in order to remove the arbitrary microstructural state originating from free uncontrolled cooling after foaming and in order to maximize strength. The zinc foams, however, were tested in the "as-foamed" state.

Composite structures consisting of aluminium tubes and an aluminium foam filling were made the following way (Fig. 4a). Tubes of foamable Al–6 wt % Si–4 wt % Cu alloy were inserted into conventional tubes made from an aluminium alloy 6061. The tubes were co-extruded in a hydrostatic extrusion machine, yielding a composite consisting of an outer tube which was coated by a layer of a foamable material on the inner wall. The bonding between foamable layer and the outer tube was metallic owing to the deformation during extrusion. The whole composite was then placed into a furnace. The temperature was controlled in a way that the outer tube remained solid while the foamable layer expanded towards the centre of the tube until the tube was entirely filled with foam. This procedure was repeated for various tubes of different wall thicknesses and various thickness of the foamable layer, leading to tubes filled with foam of different densities. Two examples of such tubes are shown in Fig. 4b. For the compression tests presented in this paper the wall thickness of the tube was 2.5 mm, the tube diameter was 30 mm and the foam densities ranged from 0.45 to 0.6 g cm^{-3}.

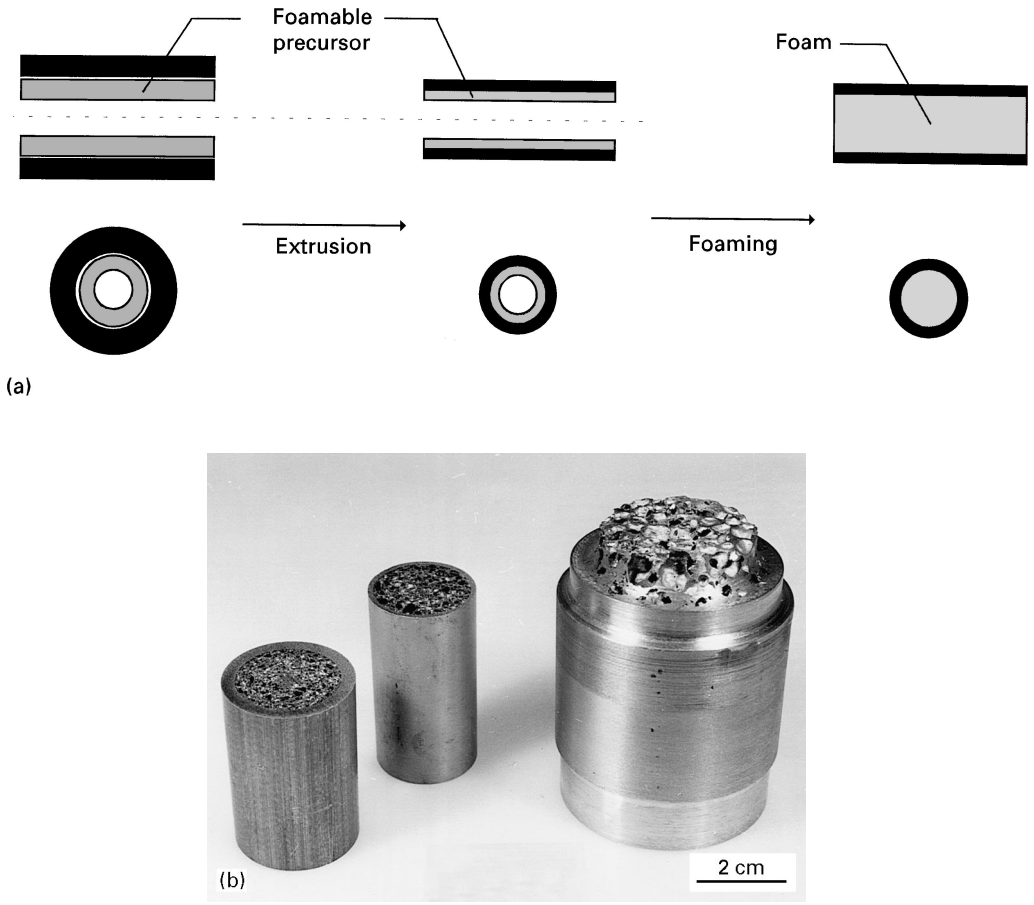

Figure 4 (a) Process for making foam-filled tubes. (b) Aluminium alloy 6061 tubes filled with Al–6 wt % Si–4 wt % Cu foam.

3. Mechanical testing of aluminium foams

3.1. Definitions

A number of metal foams having the nominal compositions Al–6 wt % Si–4 wt % Cu and Zn–4 wt % Cu were tested in quasistatic compression tests. All foams, whatever material they were made of, exhibited the universal deformation behaviour [9] which is shown in Fig. 5 in schematic form; for small compressions, one observes an increase in stress which at first sight appears to be elastic. A more thorough analysis, however, revealed that the increase is only partially reversible and that certain irreversible deformation processes of the foamed structure occur during the first loading. Young's modulus, therefore, cannot be determined by measuring the slope of the initial stress increase but has to be determined by other means such as by measurements of flexural vibrations [13]. Small-scale plastic deformations are also responsible for the mechanical damping of metal foams which is at least ten times the damping of the corresponding matrix metals [14].

After the initial increase in stress there is then a change to a regime of very strong plastic deformation characterized by a small slope of the stress–strain curve. In some cases the curve is even horizontal. Sometimes an upper and lower yield point is observed [10, 11]. After an extended plateau regime the stress–strain curve gradually changes into the regime of densification when the cell walls touch each other, accompanied by a steep increase in stress. The form of the stress–strain curve shown in Fig. 5 varies with density, density gradients and composition of the metal foam but always shows the same principal behaviour.

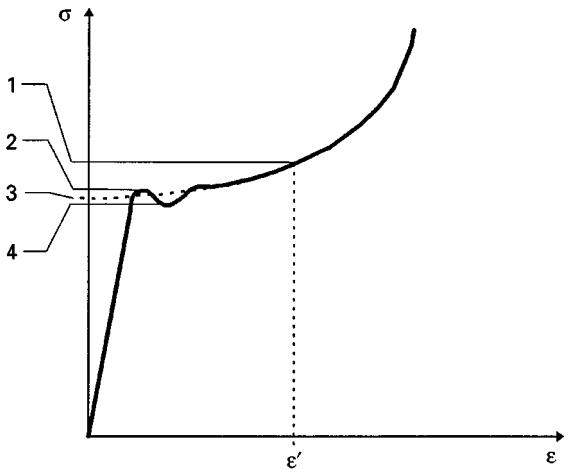

Figure 5 Schematical stress–strain diagram of a foam. The numbers denote the various compression strengths defined. 1, compression strength $\sigma_{\varepsilon'}$ at a given strain ε'; 2, upper yield strength σ_u; 3, strength σ extrapolated from the stress–strain curve in the plateau regime; 4, lower yield strength σ_l.

For the characterization of foams and the evaluation of their potential applications a determination of their compression behaviour or, more specifically, their compression strength and the length and slope of

the plateau is important. The definition of compression strength for foams, however, is not unambiguous. There are various possibilities to define this quantity. In Fig. 5 these possibilities are denoted by numbers: one can use the upper (definition 2) or lower (definition 4) yield points, σ_u and σ_l, respectively, as measure for the compression strength [10, 11] or one can use an average. In the case when no such yield points can be observed and the stress–strain curve increases sufficiently smoothly, one can extrapolate the plateau regime to $\varepsilon = 0$ and define a compression strength σ_f this way (definition 3). Finally, one can simply take the stress at a certain given deformation, e.g., 10 or 20%, and use the corresponding deformation stresses, $\sigma_{\varepsilon=10}$ or $\sigma_{\varepsilon=20}$, as compression strength (definition 1). However, the latter procedure is only suitable for smooth curves because otherwise the results will be influenced by fluctuating stresses too much. This is the case in brittle materials, for example. In the present work the extrapolation method (definition 3) was applied in most cases. In the few cases, however, where the stress drops after a first maximum (e.g., sample 14 of Fig. 12), this method cannot be used and the upper yield stress, σ_u, was used as the compression strength.

3.2. Aluminium foams

In a first series of measurements, foams of the nominal composition Al–6 wt % Si–4 wt % Cu were tested which had two closed outer surfaces originating from the foaming process and four sides where the porosity was open owing to cutting (Fig. 3). The Al–6 wt % Si–4 wt % Cu alloy was chosen because of its low melting point which facilitated the filling of aluminium tubes (see Section 3). In the compression tests the testing direction was chosen in parallel and perpendicular to the closed outer surface corresponding to the orientations in Fig. 6a and b.

The parameter varied was the overall density of the foam. In Fig. 7a and b the stress–strain curves for a number of these foam specimens are shown. As one can see easily, the orientation of the closed skin with respect to the testing direction influences the deformation characteristics in a very pronounced way. In Fig. 7a the stresses before the onset of strong plastic

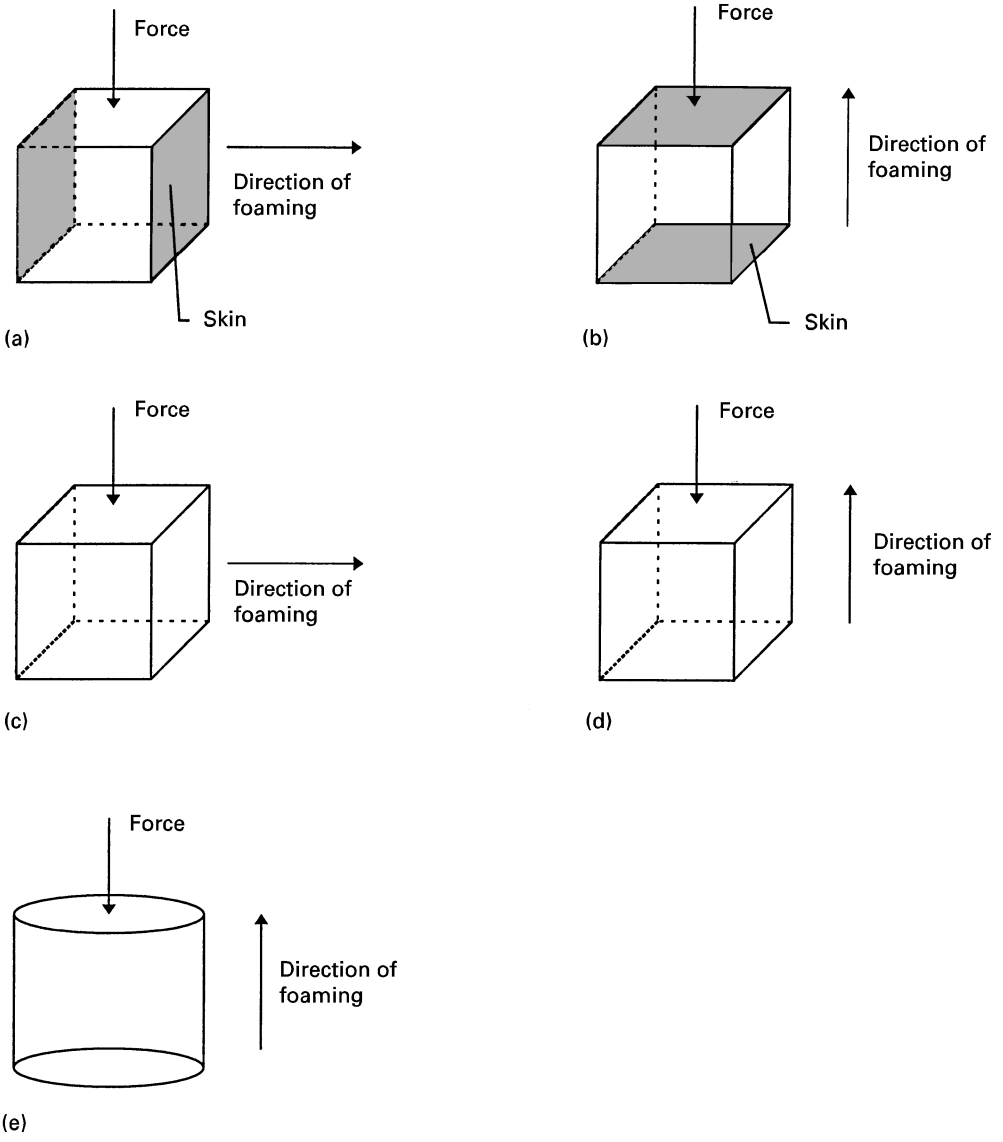

Figure 6 Testing configurations used in the investigations.

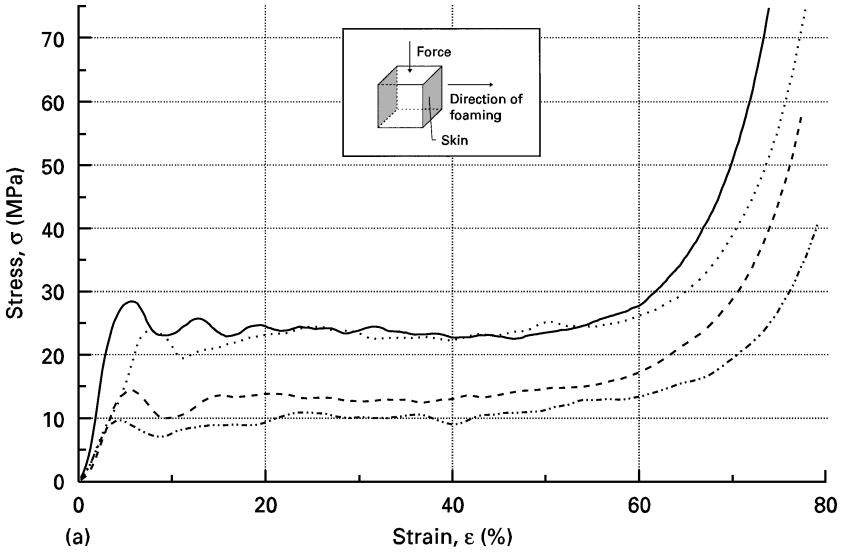

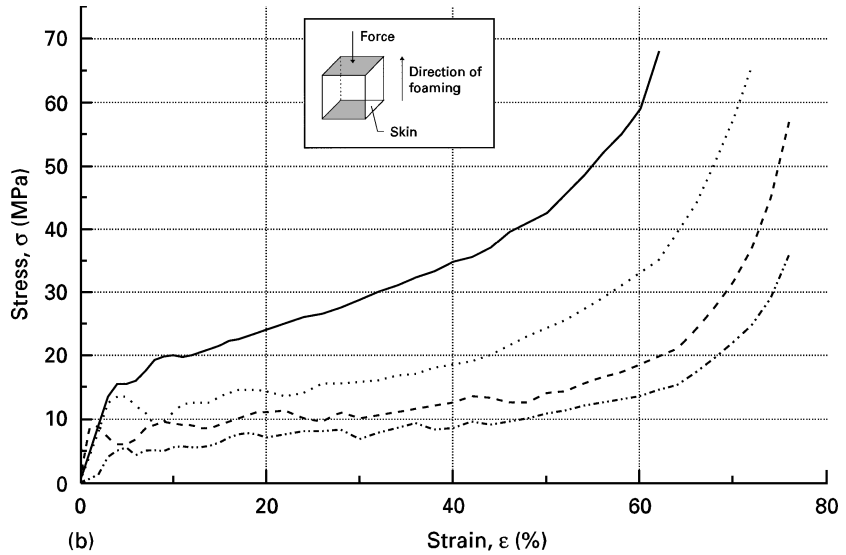

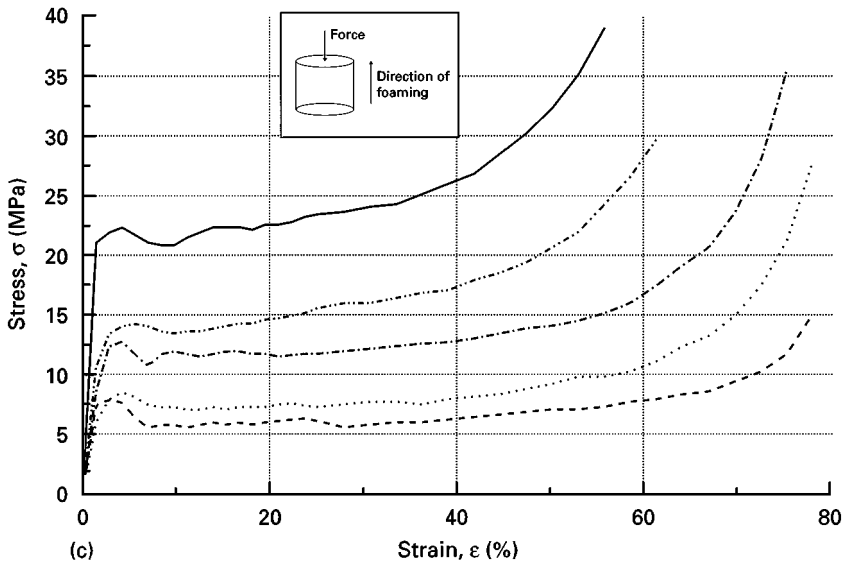

Figure 7 Stress–strain diagrams: (a) Al–6 wt % Si–4 wt % Cu oriented as in Fig. 6a ((– - - –), $\rho = 0.39\ g\,cm^{-3}$; (– – –), $\rho = 0.44\ g\,cm^{-3}$; (- - - - -), $\rho = 0.54\ g\,cm^{-3}$; (——), $\rho = 0.58\ g\,cm^{-3}$); (b) Al–6 wt % Si–4 wt % Cu oriented as in Fig. 6b ((– - - –), $\rho = 0.35\ g\,cm^{-3}$; (– – –), $\rho = 0.42\ g\,cm^{-3}$; (- - - - -), $\rho = 0.49\ g\,cm^{-3}$; (——), $\rho = 0.70\ g\,cm^{-3}$); (c) Zn–4 wt % Cu oriented as in Fig. 6e ((– – –), $\rho = 1.04\ g\,cm^{-3}$; (- - - - -), $\rho = 1.14\ g\,cm^{-3}$; (– – –), $\rho = 1.38\ g\,cm^{-3}$; (– - - –), $\rho = 1.55\ g\,cm^{-3}$; (——), $\rho = 1.95\ g\,cm^{-3}$).

deformation and therefore the compression strength are much higher than in Fig. 7b. Moreover, in the plateau regime the stress curve is nearly horizontal in Fig. 7a. In Fig. 7b, however, no range of constant stress can be observed except for the foams with very low densities.

In general it can be said that for arbitrary orientations of the outer skin the plateau regime is longer the lower that the foam densities are, but of course lower densities also imply lower absolute compression strengths. In Fig. 8 this correspondence is shown in the form of a plot of the compression strength versus the foam density. All samples were measured in the orientation shown in Fig. 6b corresponding to the data shown in Fig. 7b. The correlation between density and compression strength is obvious. Also, a relatively strong scatter of the measured strengths can be seen. This is partially due to the small size of the samples which on the average contain 15–20 pores across each sample dimension. For larger samples, one could expect a smaller scatter of the results. However, one must not forget that foams are statistical systems and therefore are always expected to show a much more pronounced scatter of their properties than conventional massive metals or alloys do.

The axes in Fig. 8 are scaled logarithmically. The reason for this is that many mechanical and physical properties of porous systems follow a power law of the form [9]

$$A(\rho) = A_0 \rho^n$$

where n is an exponent which depends on the quantity considered and A_0 is a pre-factor which reflects the properties of the matrix material and also depends on the quantity considered.

For the compression strength one expects an exponent of $n = 1.5$ for the case when the influence of the membranes can be neglected and the strength essentially comes from the struts of the cells [9]. This result was derived using a simple cubic model of the foam. The exponents measured in the present experimental work and other comparable investigations [12, 13] are all somewhat higher and range from 1.5 to 2, and under certain circumstances up to 3.

Figure 9 shows the compression strengths for an orientation of the outer skins described by the configuration in Fig. 6a. One sees that the values also follow a power law and that the exponent is in the same range as for the results shown in Fig. 8. For comparison the resulting fitted line of Fig. 8 has been included in Fig. 9, confirming what was already evident from Fig. 7a, namely that the compression strength is much higher for the orientation in Fig. 6a. The vertical bar in Fig. 9 denotes a factor of two and this is almost the ratio of the compression strengths corresponding to the two orientations.

The reason for the observed stress–strain curve of the samples with the orientation in Fig. 6a is the supporting effect of the vertically arranged densified outer foam sections, which would show a typical buckling behaviour (characterized by a high initial stress peak and a subsequent drop in the strength) without the connected foam. The combination of these outer sections with the foam results in a superposition of this buckling behaviour with the properties of the bare foam, as given in Fig. 7b, thus yielding the curves shown in Fig. 7a.

A further possible reason for the observed difference between the stress–strain curves in Fig. 7a and b was suspected to be a possible anisotropy of the foam itself. The samples corresponding to Fig. 7a were tested

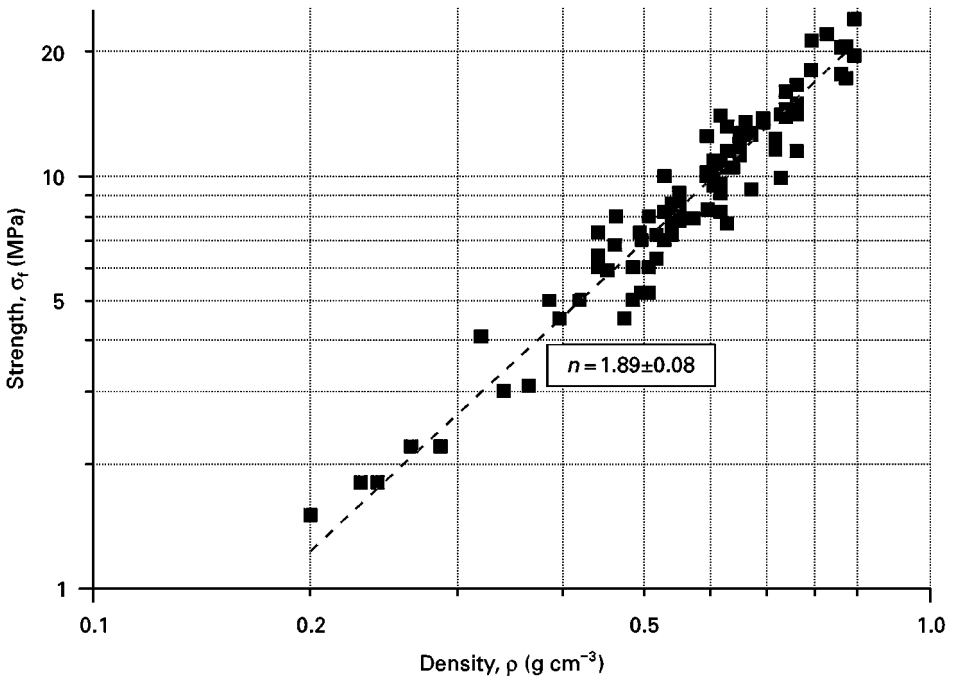

Figure 8 Compression strength of aluminium foams with skins oriented perpendicular to the testing direction. (– – –) fitted line with a slope of 1.89.

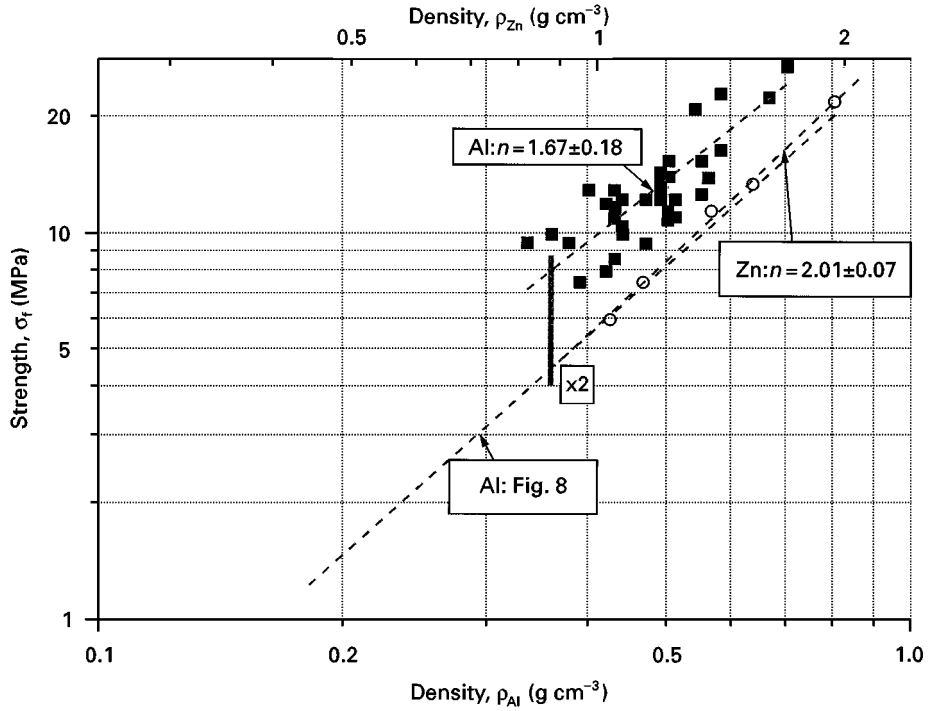

Figure 9 Compression strength of aluminium foams with skins oriented in parallel to the testing direction (■), Al; (– – –) fitted line with a slope of 1.67. For comparison the fitted line of Fig. 8 is included. Also, the compression strengths of the series of Zn–4 wt % Cu foams are shown (○), Zn, together with a corresponding fitted line with slope 2.01. The vertical bar denotes a factor of two in strength.

perpendicular to the foaming direction, and those in Fig. 7b in parallel orientation. Because of the production route used for the foamed metals which starts from a pressed semifinished product, the foaming process starts in a preferred direction. Pores are formed which are elongated in the plane perpendicular to the direction in which the powder was originally consolidated. During expansion the pores grow and become more spherical. However, possibly a slight asphericity remains, thus causing an anisotropy of mechanical properties [9]. In order to evaluate this possible influence, a series of measurements was carried out where the relative orientation of the testing and foaming direction was varied. For this, foam samples without any closed surfaces were prepared by cutting off the remaining two skins from the samples used before. The samples were tested in the two possible orientations shown in Fig. 6c and d. The resulting compression strengths are compared with each other in Fig. 10. One sees that the samples with a parallel orientation of foaming and testing direction show a slightly higher compression strength than the samples with the alternative orientation. However, the difference between the two orientations is not as pronounced as between the two skin orientations compared with each other in Figs 8 and 9 (see the corresponding vertical bars denoting a factor of two in Figs 9 and 10). The reason for the slight anisotropy is probably the deviation of pore sizes from sphericity mentioned already. The idea of this argument is depicted in Fig. 10 by strongly exaggerated schematical pore arrangements. Note that in Fig. 10 the slopes of the fitted curves cannot be determined with sufficient accuracy owing to the small number of data points. The lines in Fig. 10 should therefore be considered a guide to the eye.

3.3. Influence of heat treatment

If a metal foam is made of a metal or alloy which can be age hardened, the foam can, at least in principle, also be age hardened in order to increase its strength. Heat treatment of a metal foam, however, is not as easy as for conventional dense metallic materials. Firstly, the thermal conductivity of metal foams is reduced in comparison with that of the corresponding dense matrix material by a factor of roughly $\rho_f/3\rho_s$, where ρ_f and ρ_s are the densities of the foam and the matrix material, respectively. Also, the conductivity fluctuates locally, because of the density distribution in the foam. This causes problems when the foam has to be quenched after the initial solution annealing. The low and non-constant conductivity causes a lower quenching rate than in the corresponding dense material which also varies spatially. Therefore one cannot always suppress premature precipitation processes in the metal foam completely. Moreover, water as a medium for quenching cannot be used, because the water enters the porous structure and can partially destroy the foam. Therefore, pressurized air has to be used for quenching, thus limiting the maximum quenching rate which can be achieved. The increase in strength by a heat treatment is therefore not as pronounced for metal foams as in massive materials.

Fig. 11 shows the effect of a heat treatment of a foam made from aluminium alloy 2014. The foams were solution annealed at 500 °C for 2 h and then quenched with pressurised air. Some quenched alloys

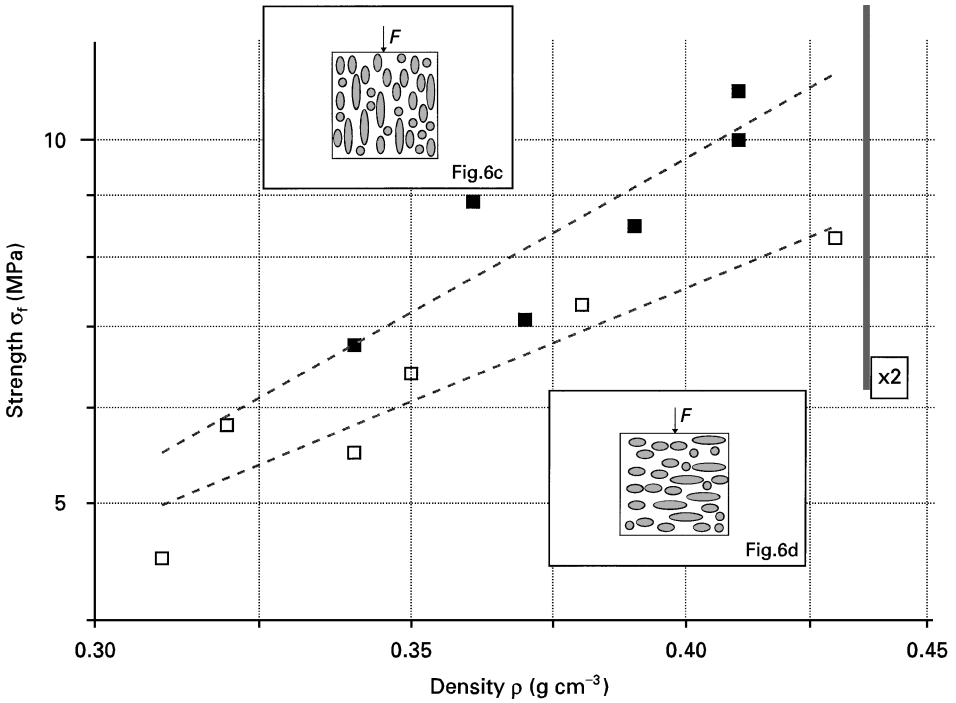

Figure 10 Compression strength of aluminium foams with the foaming direction oriented in parallel and perpendicular to the force orientation in Fig. 6c (■) and Fig. 6d (□). (– – –), fitted lines; the vertical bar denotes a factor of two.

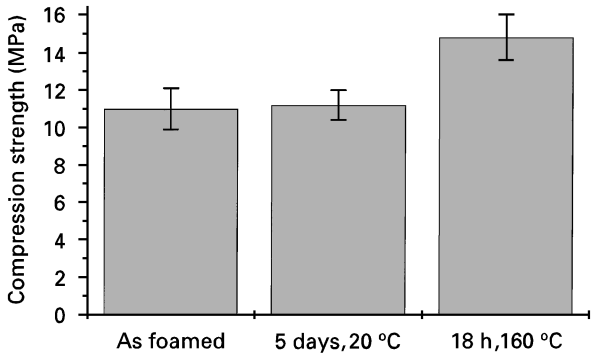

Figure 11 Effect of various heat treatments on the compression strength of aluminium alloy 2014 foams.

were tested right away without further heat treatment, some were kept at room temperature for 5 days before testing and foams of a third group were annealed at 160 °C for 18 h. The latter heat treatment is expected to yield the highest age-hardening effect. For each of the three alternatives, four foam samples of a similar density (0.6 g cm^{-3}) were chosen and an average compression strength measured. In Fig. 11 the average strength of each group of samples is compared. One sees that the samples which had the heat treatment at 160 °C show a significantly higher strength than the two other types of sample which have the same strength within the statistical error limits. Therefore, it can be concluded that the heat treatment leads to an increase in strength of about one third of the initial strength.

3.4. Zinc foams

The cylindrically shaped zinc foam samples were tested uniaxially. Fig. 7c shows a selection of five stress–strain curves. The curves are similar to those measured for aluminium foams with outer skins oriented parallel to the testing direction (Fig. 7a). Because the zinc foams also exhibited a closed skin originating from the foaming process, this behaviour is understandable. The corresponding compression strengths are compared with the aluminium foam data in Fig. 9. The upper and lower abscissa axes correspond to Zn and Al, respectively, and were normalized to relative density. One sees that the compression strength of Zn foams also follows a power law with an exponent of $n \approx 2$. The absolute strengths of the aluminium and zinc alloys are very similar in this figure, which is of course pure coincidence.

4. Testing of composite structures based on aluminium foams

For energy absorbers a stress–strain curve which comes close to the ideal rectangular shape is advantageous. Therefore, aluminium foams with outer skins oriented parallel to the force approximate the ideal shape rather well, as can be seen from Fig. 7a. The details of the deformation behaviour depend on material parameters such as the alloy composition and the density of the foam but also on the thickness of the closed skins. The thickness, however, can only be varied within a certain range by modifying the foaming conditions such as temperature and heating rate. Therefore, an attempt was undertaken to obtain a very pronounced skin effect by filling a tube with aluminium foam and testing the composite in an analogous way. Because the outer skins have a metallic bonding to the actual foam body, a configuration was desired, where the foam and the outer tube also have

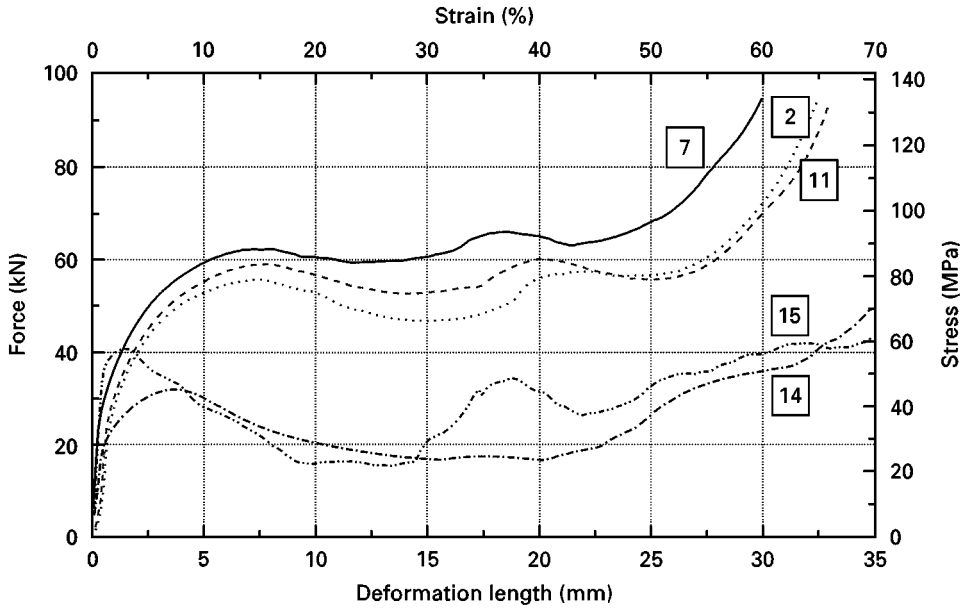

Figure 12 Stress–strain curves of axially tested aluminium tubes filled with aluminium foam. The sample numbers correspond to the foam densities: sample 2, 0.53 g cm^{-3}; sample 7, 0.57 g cm^{-3}; sample 11, 0.49 g cm^{-3}. In sample 14 the foam core has been removed prior to testing. Sample 15 was a precursor composite consisting of a tube and the foamable material.

a metallic bonding. Such samples could be produced by the method described in Section 2.

Pieces of foam-filled tube of 50 mm length were tested. However, the density of the foam filling could only be varied between 0.45 and 0.65 g cm^{-3}. Some resulting stress–strain curves are shown in Fig. 12. Also shown are curves corresponding to a precursor composite tube, consisting of an outer tube and the inner foamable layer, and to a tube where the foam had been removed prior to testing.

An obvious feature is the occurrence of a nearly horizontal plateau up to 50–55% strain and a very high plateau stress ranging from 80 to 90 MPa. The formation of folds in the outer tube is reflected by the slight stress modulations during compression. Compared with the precursor material and with the tube without foam the foam-filled tube shows a much higher strength and a better and longer plateau regime. The composite therefore has mechanical strengths which are higher than the sum of the strengths of the single components. A reason for this is that the foam filling increases the stability of the profile by preventing the profile from buckling. This explains the higher yield point. After buckling has started, parts of the foam filling will be compressed in the various folds and this way make further compression more difficult.

5. Technological outlook

Up to the present day, only polymer foams or honeycomb structures are actually applied in light-weight construction or energy-absorbing devices. The possibility of tailoring the stress–strain behaviour of such materials by choosing an appropriate matrix material, density or cell orientation makes these structures nearly ideal for such applications. Metal foams could help to enlarge the spectrum of application for foams and porous materials in general because of their high strength and other properties which originate from the metallic nature of the matrix material.

Decisive for the quality of packing protections or energy absorbers is the ability to absorb large amounts of energy without exceeding a given stress level which would lead to damage or injury. Metal foams can be superior to polymer foams where, owing to limited space, higher deformation stresses combined with an equal or better energy absorption behaviour is required.

A result of the investigations presented here is that a simple piece of foam does not necessarily represent an optimum energy absorber. Foams with closed outer skins (structural foams) or composite structures of profiles and foams can have a deformation behaviour which makes them more suitable for such applications.

6. Summary

Mechanical tests of metal foams under uniaxial compression showed that the form of the stress–strain diagram depends on the density of the foam, on the relative orientation of the testing and foaming direction, and on the orientation of closed outer skins. Higher densities in general lead to higher stresses under compression conditions but also to a reduction in the range of the technologically important plateau regime. A parallel orientation of the outer skins with respect to the applied force leads to a higher strength and to an extension of the plateau regime compared with the perpendicular orientation. The relative orientation of force and foaming direction, however, is of minor importance. The foams investigated are therefore nearly isotropic. The observed influence of closed and densified outer skins is comparable with the behaviour of foam with a high plateau stress. The optimization of such structures will be the subject of future work.

References

1. J. BANHART (ed.), in Proceedings of the Conference on Metal Foams, Bremen, 6–7 March 1997 (MIT Publications, Bremen, 1997) (mostly in German).
2. W. W. RUCH and B. KIRKEVAG, PCT/WO Patent 91/01387 (1991).
3. I. JIN, L. D. KENNY and H. SANG, US Patent 4 973 358 (1990).
4. J. BAUMEISTER, DE Patent 40 18 360 (1991).
5. *Idem*., US Patent 5 151 246 (1992).
6. J. BAUMEISTER and H. SCHRADER, DE Patent 41 01 630 (1992).
7. J. BAUMEISTER, J. BANHART and M. WEBER, DE Patent 43 25 538 (1996).
8. J. BANHART, J. BAUMEISTER and M. WEBER, in Proceedings of the European Conference on Advanced PM Materials, Birmingham, UK, 23–25 October 1995 (European Powder Metallurgy Association, Shrewsburg, 1995) p. 201.
9. L. J. GIBSON and M. F. ASHBY, Cellular solids (Pergamon, Oxford, 1988).
10. P. H. THORNTON and C. L. MAGEE, *Metall. Trans. A* **6** (1975) 1253.
11. *Idem*., *Ibid*., **6** (1975) 1801.
12. M. WEBER, J. BAUMEISTER and J. BANHART, in Proceedings of the Powder Metallurgy World Congress, Paris, 1994, (Les Editions de Physique, Les Ulis, 1994) p. 585.
13. J. BANHART, J. BAUMEISTER and M. WEBER, *VDI-Ber*. **1021** (1993) 277.
14. *Idem*., *Mater. Sci. Engng* **A205** (1996) 221.

Received 28 May
and accepted 12 November 1997